Int. J. Peptide Protein Res. **36**, 1990, 147–155

Conformations of disulfide bridges in proteins

N. SRINIVASAN, R. SOWDHAMINI, C. RAMAKRISHNAN and P. BALARAM

Molecular Biophysics Unit, Indian Institute of Science, Bangalore, India

Received 6 December 1989, accepted for publication 28 January 1990

The conformational characteristics of disulfide bridges in proteins have been analyzed using a dataset of 22 protein structures, available at a resolution of $\leqslant 2.0$ Å, containing a total of 72 disulfide crosslinks. The parameters used in the analysis include (ϕ, ψ) values at Cys residues, bridge dihedral angles χ_{SS}, χ_i^1, χ_j^1, χ_i^2, and χ_j^2, the distances C_i^α-C_j^α and C_i^β-C_j^β between the C^α and C^β atoms of Cys(i) and Cys(j). Eight families of bridge conformations with three or more occurrences have been identified on the basis of these stereochemical parameters. The most populated family corresponds to the "left handed spiral" identified earlier by Richardson ((1981) *Adv. Protein Chem.* **34**, 167–330). Disulfide bridging across antiparallel extended strands is observed in α-lytic protease, crambin, and β-trypsin and this structure is shown to be very similar to those obtained in small cystine peptides. Solvent accessible surface area calculations show that the overwhelming majority of disulfide bridges are inaccessible to solvent.

Key words: cystine residues; disulfide bonds; disulfide conformation; protein conformation; protein data analysis

Disulfide bridges are widely found in proteins and can act as important structural elements (1, 2) and also play a crucial functional role in proteins involved in redox processes (3, 4). The introduction of disulfide bonds into proteins by site-directed mutagenesis (5), as a means of stabilizing the native folded state, has been explored in the cases of T4 lysozyme (6, 7), subtilisin (8, 9) and dihydrofolate reductase (10, 11). Disulfides formed between appropriately positioned cysteine residues have also been used as a covalent crosslink, to stabilize intersubunit interactions in DNA binding proteins like λ-repressor (12). Disulfide bridges are also frequently observed in low molecular weight biologically active peptides, where they undoubtedly play a key role in stabilization of conformations important for activity. Examples include oxytocin (13), vasopressin (13), conotoxin (14), endothelin (15) and enterotoxin (16). Disulfides in peptides and proteins have been the focus of several stereochemical investigations and recent interest has centred on computer modelling as a means of identifying appropriate positions for "engineering" S-S bridges into proteins of known crystal structure (17, 18). As part of a program for modelling S-S bridges, we have carried out a detailed analysis of the stereochemistry of disulfide bridges in proteins, for which crystal structures have been reported to a resolution of $\leqslant 2.0$ Å. A total of 22 independent protein structures, containing 72 disulfide bridges, has been used for the data analysis. The results permit identification of several different families of disulfide bridge conformations, extend previous analyses based on more limited data (1, 19), and provide good stereochemical parameters for modelling studies.

METHODS

Coordinates of protein crystal structures containing disulfide bonds, refined at a resolution of $\leqslant 2.0$ Å, were obtained from the Protein Data Bank (20). Only one member of each family of structurally, highly homologous proteins (cf. papain/actinidin, human lysozyme/HEW lysozyme, β-trypsin, BPTI/trypsin-trypsin inhibitor complex) was chosen for inclusion in the analysis. A list of the proteins included in the data set, together with the relevant literature citations, is presented in Table 1. The stereochemical parameters of interest in analyzing cystine bridges are defined in Fig. 1.

Solvent accessible surface area (ASA) calculations were performed using a program kindly supplied by Prof. F.M. Richards (Yale University). The van der Waals radii used for various atoms are as suggested by Bondi (43) and used by Lee & Richards (44). The

TABLE 1

List of proteins used for the analysis

Protein[a]	PDB code	Resolution Å	R Factor[c]	No. of disulfides considered	Ref. No.
Alpha-lytic protease	2ALP	1.7	0.131	3	21
Azurin	2AZA	1.8	0.157	2	22
Bence-Jones protein (lambda, variable domain)	2RHE	1.6	0.149	1	23
Bence Jones protein (REI variable domain)	1REI	2.0	—	1	24
Crambin	1CRN	1.5	0.104	3	25
Carboxypeptidase A	5CPA	1.54	—	1	26
Erabutoxin	2EBX	1.4	0.22	4	27
Glutathione reductase	3GRS	1.54	0.186	1	28
Immunoglobulin FAB	1FB4	1.9	0.189	6	29
Insulin[b]	1INS	1.5	0.179	3	30
Lysozyme (Human)	1LZ1	1.5	0.177	4	31
Ovomucoid third domain	2OVO	1.5	0.199	3	32
Papain	9PAP	1.65	0.161	3	33
Pencillopepsin	2APP	1.8	0.126	1	34
Phospholipase A2	1BP2	1.7	0.171	7	35
Proteinase A	2SGA	1.5	0.126	2	36
Rat mast cell protease	3RP2	1.9	0.191	6	37
Ribonuclease A	5RSA	2.0	0.159	4	38
Scorpion neurotoxin	1SN3	1.8	—	4	39
Trypsin inhibitor	5PTI	1.0	0.200	3	40
Trypsin complex with *p*-amidino phenyl pyruvate	1TPP	1.4	0.191	6	41
Wheat germ agglutinin[b]	3WGA	1.8	0.179	4	42

[a] Out of 66 independent protein structures solved at ≤ 2 Å resolution, only 27 contain disulfide bonds. In this study, of the homologous proteins (cf. actinidin and papain, HEW lysozyme and human lysozyme) only one of them has been considered. Most of the toxins and proteases have been considered, since their homology and disulfide bond stereochemistry vary.

[b] In cases of proteins occurring as multimers or made up of structurally similar subunits or in the case of more than one molecule in the asymmetric unit (cf. insulin and wheat germ agglutinin), only one set has been considered.

[c] Proteins whose R factor has not been reported in the protein data bank carry a "—" mark against the R factor.

radius of the probe (water) molecule used was 1.4 Å. The sum of the ASA of C^{β} and S^{γ} atoms in protein disulfides is compared with that in an isolated, hypothetical model. The model systems chosen consist of two Gly-Cys-Gly segments in the extended "silk" conformation ($\phi = -140°, \psi = 135°$) (1), with a disulfide crosslink. Two sets of sidechain conformations were used, representing left- and right-handed disulfides. These are characterized by the following torsion angles: (a) $\chi_{ss} = -90°$, $\chi_i^1 = \chi_j^1 = \chi_i^2 = \chi_j^2 = -60°$ and (b) $\chi_{ss} = 90°$, $\chi_i^1 = \chi_j^1 = -60°$ and $\chi_i^2 = \chi_j^2 = -90°$. These values correspond to preferred conformations in proteins. The sum of the ASA values of C^{β} and S^{γ} atoms for the model left- and right-handed disulfides are 91.5 Å^2 and 112.6 Å^2, respectively. The percentage ASA for protein disulfides is expressed relative to the appropriate model.

RESULTS AND DISCUSSION

A total of 72 disulfide bridges have been examined out of which 69 are intrachain disulfides, while 3 crosslink two separate polypeptide chains. The number of inter-

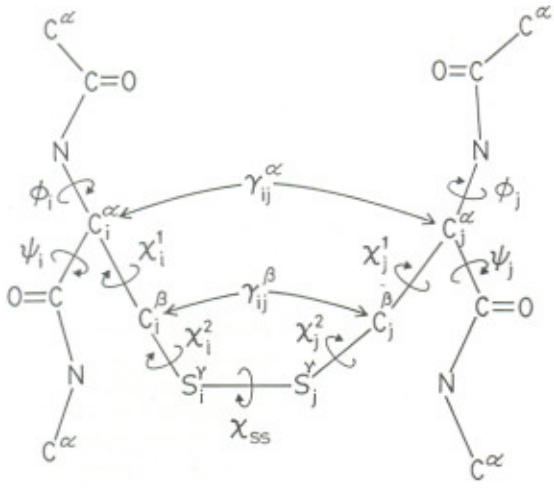

FIGURE 1

Conformational parameters characterizing disulfide bridge stereochemistry.

vening amino acids between the two linked Cys residues varies from 4 to 129. There are two peaks in the distribution of loop sizes viz. a broad peak between 10 and 30 residues (31 examples) and a sharp peak between 60 and 70 residues (10 examples).

Backbone conformations at disulfide bridges

Fig. 2a shows the distribution of backbone torsional angles (ϕ, ψ) at all the non-Gly residues in the 22 proteins examined, represented on a Ramachandran map (45). The distribution observed for the Cys residues in these proteins is shown in Fig. 2c. The population distributions in (ϕ, ψ) space in the two cases are shown as a grid representation in Fig. 2b and d. Clearly there is no difference observed in the statistical distribution of backbone conformations observed for the Cys residues involved in disulfides as compared to the other residues, in the data set being studied. A similar analysis carried out for the residues preceding and succeeding the Cys residues did not reveal any unusual distribution of (ϕ, ψ) angles in the vicinity of S-S bridges, although a small cluster of points in the right handed side of the (ϕ, ψ) map ($\phi \sim +50°$, $\psi \sim +40°$) was observed for the residues preceding Cys in the bridge. A slight preponderance of residues in the extended regions of (ϕ, ψ) space ($\phi \sim -90°$, $\psi \sim +140°$) is observed for the Cys residues as well as the other residues. Of the 72 disulfides examined, 23 linked regions of extended β-strands, 4 linked helices and 12 connected helical segments to β-strands. Six Cys residues involved in disulfide bridges were found to occur in β-turns (2 at the i + 1 position, 3 at the i + 2 position, and 1 in multiple bends). While the observations suggest a preference for S-S bridges connecting two extended strands, a large fraction of the observed bridges linked two irregular segments of the polypeptide chain.

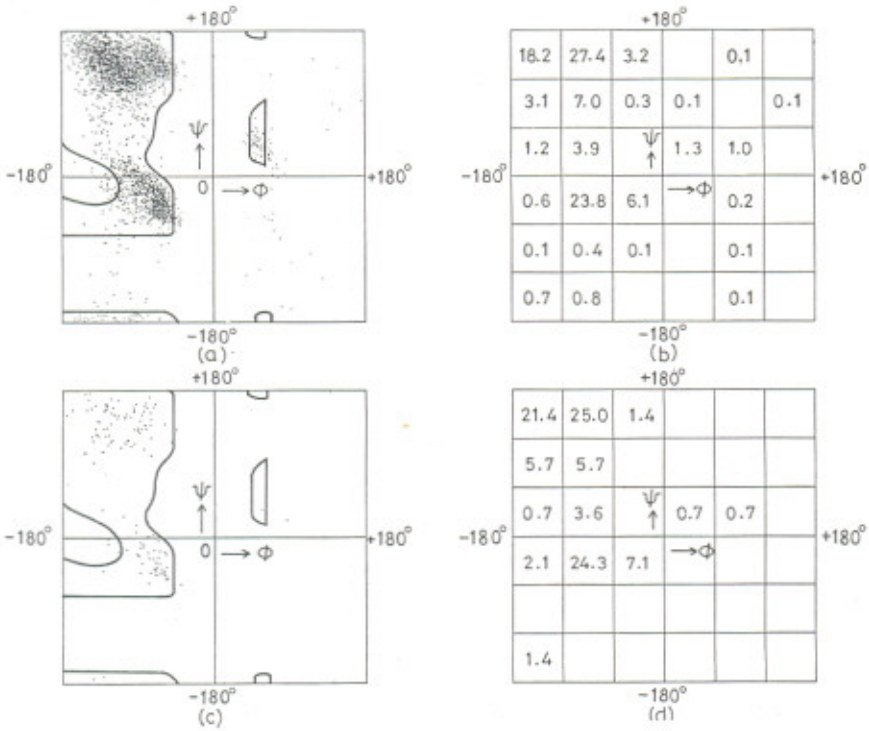

FIGURE 2

(a) (ϕ, ψ) plot of 3564 non-Gly residues in 22 proteins (Table 1), superimposed on the Ramachandran steric map for an L-alanyl residue. "Stereochemically allowed" regions are enclosed by dark lines. (b) Distribution of amino acid conformations in (ϕ, ψ) space represented on a grid drawn at 60° intervals. Data is taken from (a) and the numbers represent the percentage of residue conformations that occur in that grid. Only non-zero values are shown. (c) and (d) Data for 140 disulfide bonded Cys residues in 22 proteins represented as in plots (a) and (b) respectively. Note: Of the 72 disulfide bonded pairs of Cys residues analyzed, four Cys residues occur at the *C*-termini and have been omitted from the (ϕ, ψ) plot.

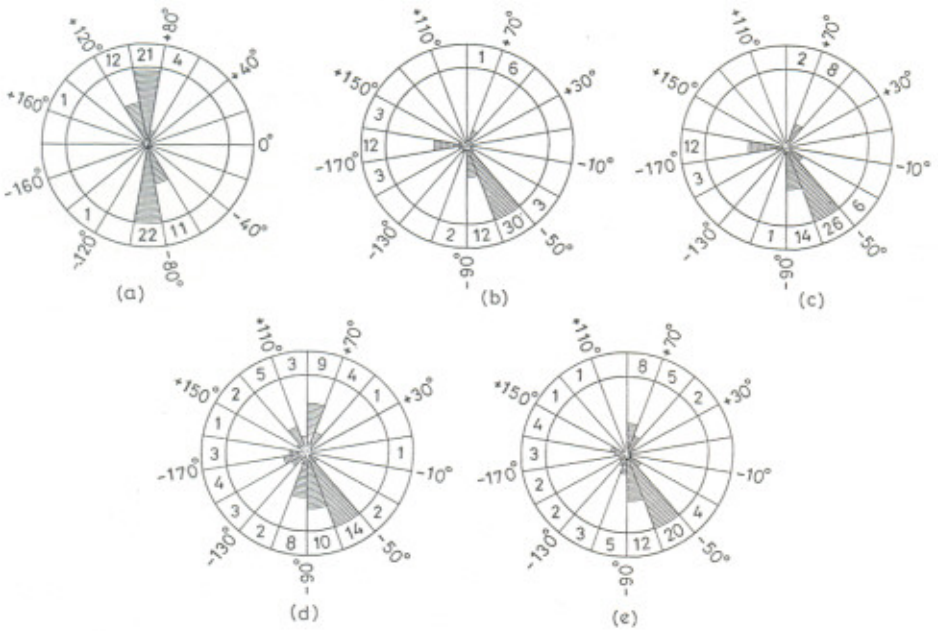

FIGURE 3

Distribution of disulfide bridge dihedral angles in 72 disulfides represented as circular plots. The radial lengths of the shaded areas are proportional to the number of occurrences. Number of occurrences are indicated at the top or bottom of each sector. The angular scale is indicated on the outer circle. (a) χ_{SS}, (b) χ_i^1, (c) χ_j^1, (d) χ_i^2, and (e) χ_j^2. Only non-zero values are shown.

Disulfide bridge conformational parameters

The observed distributions of the five bridge torsion angles χ_{SS}, χ_i^1, χ_j^1, χ_i^2, and χ_j^2 (Fig. 1 for definition) are shown in a circular plot representation in Fig. 3. As expected, the most populated χ_{SS} values lie in the ranges $+90° \pm 20°$ and $-90° \pm 20°$, corresponding to right- and left-handed disulfide conformations. χ_i^1 and χ_j^1 values are clustered about the expected values of $-60°$, $60°$, and $180°$, corresponding to the three staggered orientations about the $C^\alpha—C^\beta$ bond. A large majority of the χ^1 values are close to $-60°$. The distribution of χ_i^2, χ_j^2 values is less well defined and there is a broader spread. However, two distinct clusters near $\chi_i^2 \sim -70°$ and $\chi_j^2 \sim 80°$ are observed.

The distributions of the distances C_j^α-C_j^α (r_{ij}^α) and C_i^β-C_j^β (r_{ij}^β) are shown as histograms in Fig. 4. There is a fairly large spread of r_{ij}^α (3.8–6.8 Å) with clusters noticed at 5.0 Å, 5.8 Å, and 6.2 Å. r_{ij}^α values have been classified into three groups viz. small (S) 3.8–4.8 Å, medium (M) 4.8 Å $< r_{ij}^\alpha <$ 5.8 Å, and large (L) $>$ 5.8 Å for purposes of further analyzing specific bridge conformations. The large r_{ij}^α values are mostly derived from immunoglobulin structures. The r_{ij}^β values occur over a narrow range of 3.5–4.5 Å, with the majority (81%) lying between 3.6 and 4.0 Å. A further classification of these distances into three groups, viz.

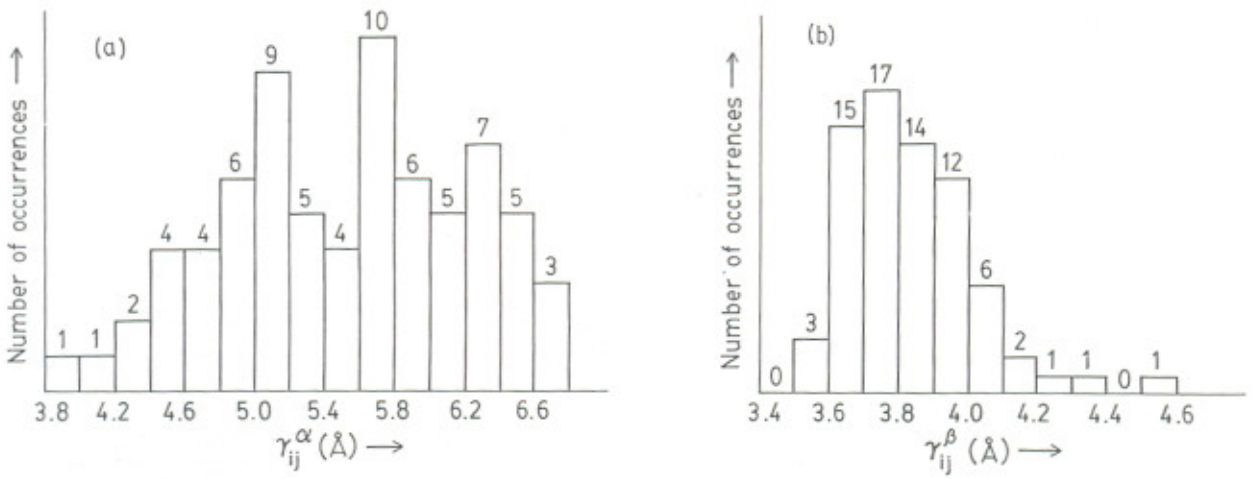

FIGURE 4

Histograms showing the distributions of the distances (a) C_i^α-C_j^α (r_{ij}^α) and (b) C_i^β-C_j^β (r_{ij}^β) in 72 disulfides.

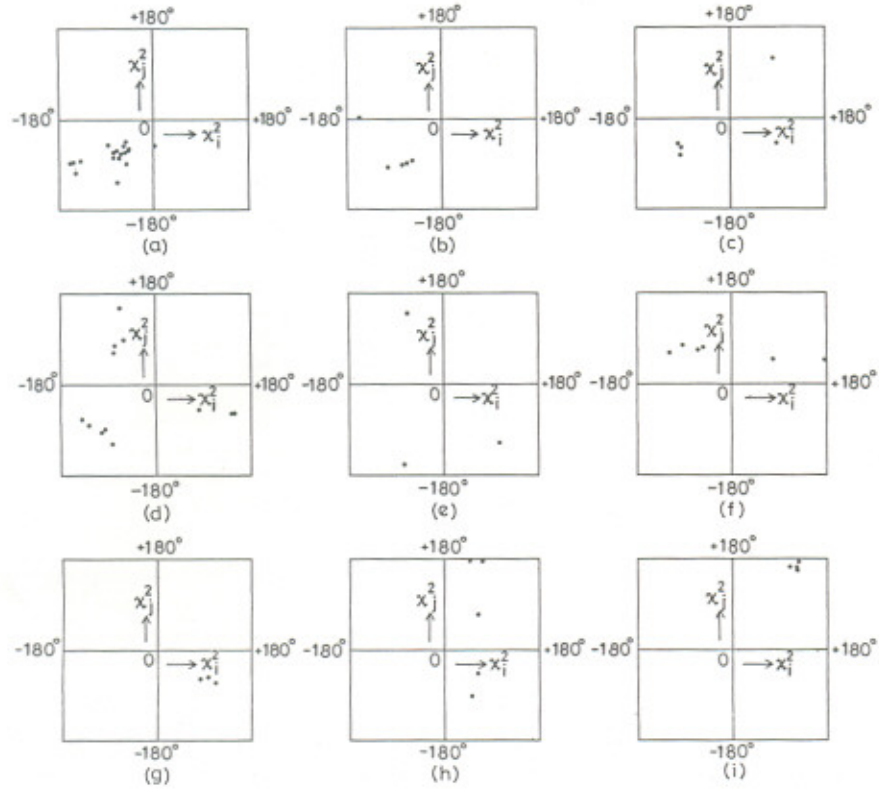

FIGURE 5

(χ_i^2, χ_j^2) plots for the following combinations of χ_{ss}, χ_i^1 and χ_j^1: ($\chi_{ss} \sim 90°$ p; $\chi_{ss} \sim -90°$ n; χ_i^1 or $\chi_j^1 \sim 60°$ g$^+$; χ_i^1 or $\chi_j^1 \sim -60°$ g$^-$; χ_i^1 or $\chi_j^1 \sim 180°$ t) (a) ng$^-$ g$^-$, (b) ng$^-$ t, (c) ntg$^-$, (d) pg$^-$ g$^-$, (e) pg$^-$ g$^+$, (f) pg$^-$ t, (g) pg$^+$ g$^-$, (h) ptg$^-$, (i) ptg$^+$.

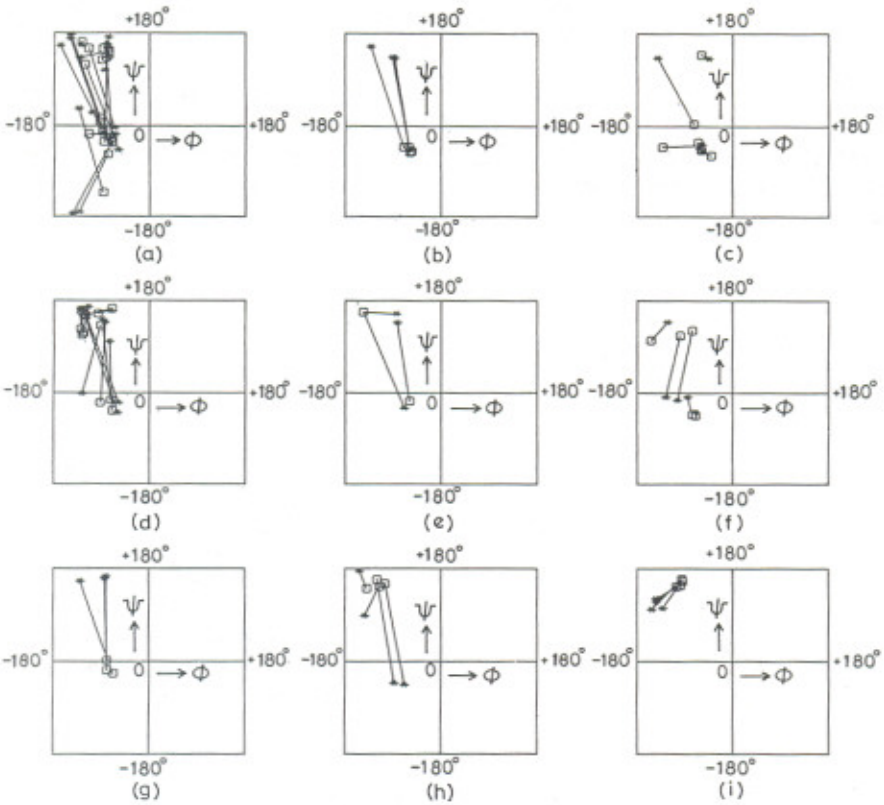

FIGURE 6

(ϕ_i, ψ_i), (ϕ_j, ψ_j) distributions corresponding to conformations shown in Fig. 5, represented by lines connecting (ϕ_i, ψ_i) * and (ϕ_j, ψ_j) □.

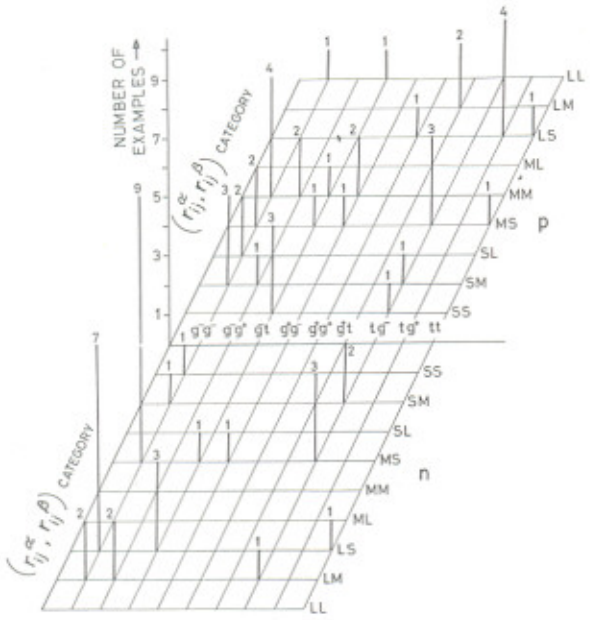

FIGURE 7

Three-dimensional plot showing the distribution of 72 disulfides with respect to χ_{SS}, (χ_i^1, χ_j^1) and (r_{ij}^{α}, r_{ij}^{β}). r_{ij}^{α} and r_{ij}^{β} are categorized as small (S), medium (M), and large (L), as described in the text. χ_i^1, χ_j^1 values are classified as g^- ($\sim -60°$), g^+ ($\sim +60°$), and t ($\sim \pm 180°$). The upper and lower halves of the diagram correspond to positive (p, $\chi_{SS} \sim +90°$) and negative (n, $\chi_{SS} \sim -90°$) chiralities of the disulfide bond.

small (S) 3.5–3.85 Å, medium (M) $3.85 < r_{ij}^{\beta} < 4.18$ Å and large (L) > 4.18 Å has been made to facilitate further analysis.

Conformational types

The data set was sorted into two groups having opposite disulfide chirality, viz. $\chi_{SS} \sim 90°$ (p, positive) and $\chi_{SS} \sim -90°$ (n, negative). 38 examples are of the p chirality, while 34 belong to the n type. The data set was further subdivided into 9 groups, corresponding to the values of $-60°$, 60°, and 180° for χ_i^1 and χ_j^1. The observed χ_i^2, χ_j^2 values for these 18 groups (9n, 9p) were represented on two-dimensional χ_i^2, χ_j^2 plots. Fig. 5 shows 6 sets of plots for positive χ_{SS} values and 3 sets of plots for negative χ_{SS} values. Data has been shown only for cases having three or more examples. The χ_i^2, χ_j^2 plots in Fig. 5 permit identification of specific clusters, characterizing similar disulfide bridge conformations. Table 2 lists the various types of bridge conformations observed, in terms of idealized values for the 5 torsion angles. For the p chirality, examples occur in the data set of all 9 combinations of χ_i^1, χ_j^1 values, although there is only one example of $\chi_i^1 \sim 60°$, $\chi_j^1 \sim 60°$ and two examples each of $\chi_i^1 \sim 60°$, $\chi_j^1 \sim 180°$; and $\chi_i^1 \sim 180°$, $\chi_j^1 \sim 180°$. In the case of n chirality no examples have been observed for the following cases: $\chi_i^1 \sim 60°$, $\chi_j^1 \sim 60°$; $\chi_i^1 \sim 60°$, $\chi_j^1 \sim 180°$; and $\chi_i^1 \sim 180°$, $\chi_j^1 \sim 60°$. Only one example has been observed for the cases $\chi_i^1 \sim 60°$,

TABLE 2

Preferred values for side-chain torsion angles

Sl. No.	Approximate values of side-chain torsion angles				
	χ_{SS} (°)	χ_i^1 (°)	χ_j^1 (°)	χ_i^2 (°)	χ_j^2 (°)
1	−90	−60	−60	−60	−60
2	−90	−60	180	−90	−90
3	−90	180	−60	−95	−60
4	+90	−60	−60	−70	+75
5	+90	−60	−60	−100	−80
6	+90	−60	180	−80	+70
7	+90	+60	−60	+100	−60
8	+90	180	+60	+120	+165
9	+90	180	−60	+60	180[a]

[a] χ_j^2 values vary over a wide range in this case. Only two of the five disulfides have χ_j^2 values close to 180° (see Fig. 5h).

TABLE 3

Stereochemical parameters for eight disulfide families

Family No.	χ_{SS} (°)	χ_i^1 (°)	χ_j^1 (°)	r_{ij}^{α}	r_{ij}^{β}	No. of examples	Remarks
1	−90	−60	−60	M or L	S	16	Left-handed spiral
2	+90	−60	−60	S	M or L	5	Bridging across anti-parallel β-strands
3	+90	−60	−60	M	M	4	All independent disulfides
4	−90	−60	180	M or L	S	4	Cys(i) in extended strand Cys(j) in helix
5	+90	−60	180	S or M	S	4	All independent disulfides
6	−90	180	−60	M	S	3	Cys(i) in helix Cys(j) in helix
7	+90	180	−60	M	S	3	All independent disulfides. Cys(j) in extended strands
8	+90	180	+60	L	S	4	Immunoglobulin family

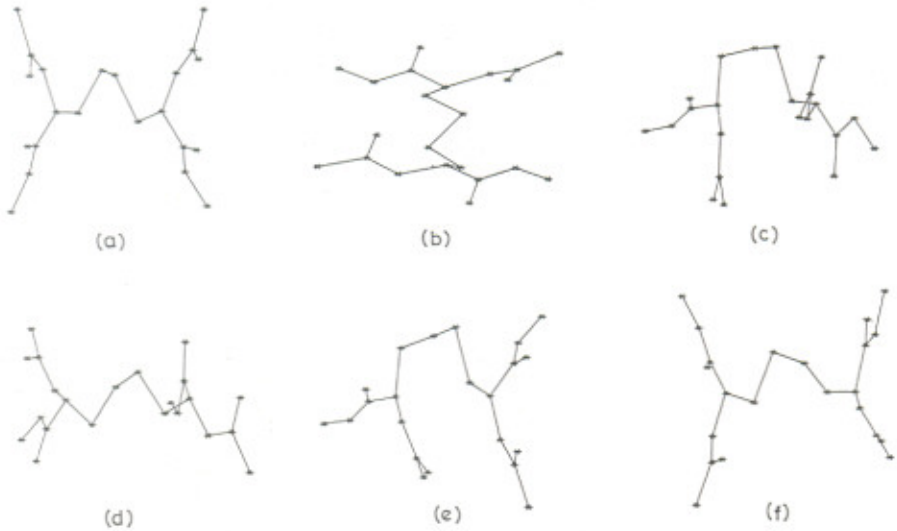

FIGURE 8
Examples of each of six major disulfide families, identified in Table 3, observed in protein structures. (a) 40–95 of ribonuclease A (5RSA), (b) 4–32 of crambin (1CRN), (c) 249–283 of pencillopepsin (2APP), (d) 30–51 of bovine pancreatic trypsin inhibitor (5PTI), (e) 56–95 of papain (9PAP), (f) 22–89 of Rhee Bence Jones protein (2RHE). In each structure, the peptide units on either side of the Cys C^{α} atoms are shown.

$\chi_j^1 \sim -60°$ and $\chi_i^1 \sim 60°$, $\chi_j^1 \sim 180°$, while two cases are observed for $\chi_i^1 \sim -60°$, $\chi_j^1 \sim 60°$. In order to establish whether a disulfide bridge conformational type correlates with the backbone conformations, at the two linked Cys residues, line diagrams in (ϕ, ψ) space $(\phi_i, \psi_i \rightarrow \phi_j, \psi_j)$ were plotted (Fig. 6) for all the nine cases represented in Fig. 5. Clear correlations are visible for several disulfide conformational types.

Identification of structural families

Disulfide bridges have been grouped on the basis of the interatomic distances r_{ij}^{α}, r_{ij}^{β} (small, medium, large) and the torsion angles χ_{SS} (positive p or negative n), χ_i^1 and χ_j^1 ($\sim -60° g^-$, $\sim 60° g^+$, $\sim 180° t$). The observations are graphically summarized in Fig. 7. Eight families with three or more occurrences are identified in Table 3. Perspective views of the six most populated disulfide conformations are shown in Fig. 8. The most populated family belongs to the "left-handed spiral" conformation identified in an earlier analysis of protein disulfides by Richardson (19). The "right-handed hook" conformation ($\chi_i^1 = -60°$, $\chi_i^2 = +120°$, $\chi_{SS} = +90°$, $\chi_j^i = -60°$, $\chi_j^2 = -50°$) also identified by Richardson is appreciably less populated and only two examples were classified as such in the data set. An interesting group of conformations belong to the $pg^- g^-$ set. These are characterized by very short r_{ij}^{α} values (3.8–4.6 Å) and correspond to disulfide bridging across the nearest residues on two "in register" antiparallel β-strands. This disulfide conformation is observed for bridge 137–159 in α-lytic protease (Fig. 9a) and also for disulfides 4–32 in crambin and 136–201 in β-trypsin (see Fig. 9b for a superposition of the disulfide bridge structures in these cases). The earlier analysis by Richardson (19) had, in fact, suggested that bridging across the nearest neighbour positions of two antiparallel β-strands is stereochemically unlikely. However, recent crystal structure analyses of model cystine peptides, Boc-Cys-Val-Aib-Ala-Leu-Cys-NHMe (46) and

the antiparallel dimer bis[Boc-Cys-Ala-Cys-NHMe] (47), have provided clear evidence for disulfide bridging across antiparallel β-sheets. Indeed, the bridge conformation in these peptides is almost identical to that observed in the proteins. A superposition of the bridge structure in the peptides with that in α-lytic protease is shown in Fig. 9d.

Solvent accessibility

The sum of the accessible surface areas computed by the method of Lee & Richards (44) for the C^{β} and S^{γ} atoms in a protein disulfide has been compared with one of two model disulfides. The models consist of two Gly-Cys-Gly segments in the silk conformation ($\phi = -140°$, $\psi = 135°$), with an S-S crosslink between them. Two sets of model structures corresponding to positive (p) and negative (n) χ_{SS} values have been used as standards for right and left handed disulfides, respectively (see Methods). Fig. 10 shows a histogram of the % accessible surface area calculated for the 72 disulfides examined. Clearly, most bridges are largely inaccessible to solvent and buried, a feature noted in the earlier analysis by Thornton (1). The only disulfides showing an appreciable ($\geqslant 50\%$) degree of solvent exposure are the bridges 14–38 in bovine pancreatic trypsin inhibitor (5PTI), 138–161 in carboxypeptidase A (5CPA), A7–B7 in insulin (1INS), 137–159 in α-lytic protease (2ALP), 58–63 in glutathione reductase (3GRS), and L 213–H 221 in immunoglobulin FAB (1FB4). Interestingly, the solvent exposed 58–63 disulfide in glutathione reductase constitutes the redox active site of the protein.

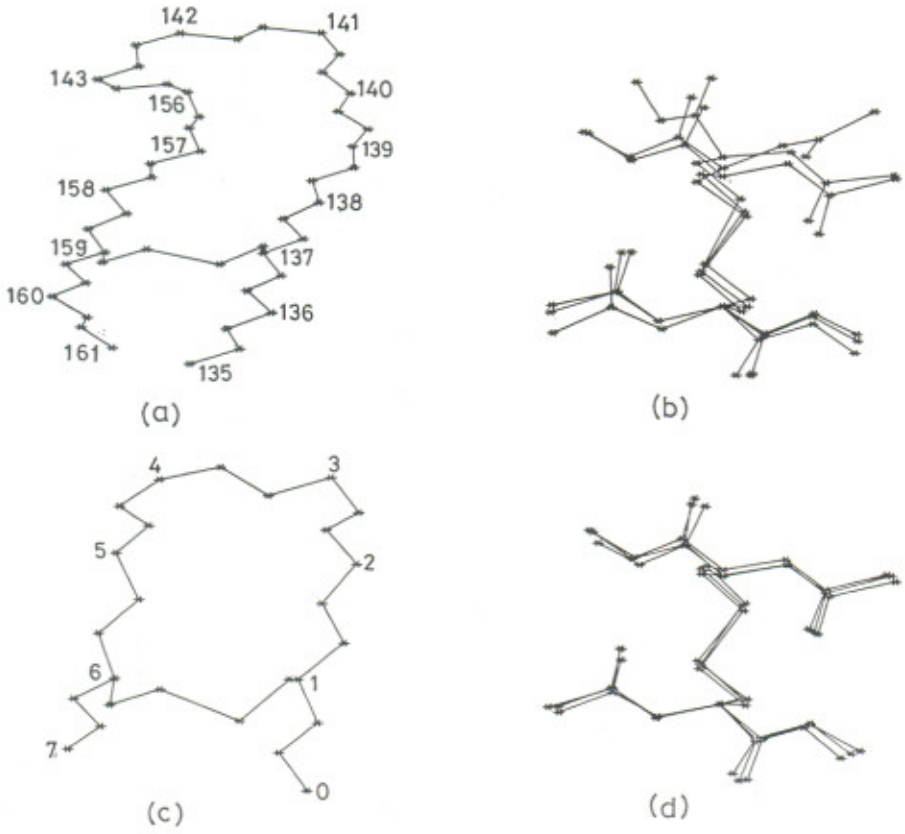

FIGURE 9

Examples of disulfide bridging across β-strand conformations. (a) Structure showing the 137–159 segment of α-lytic protease (2ALP). (Note: Discontinuity in residue numbering between 143 and 156 in the protein data bank file permits homology comparison.) N, C^{α}, C′ atoms for all the residues are shown. For the residues, 137 and 159 sidechain atoms (disulfide bridge) are also shown. C^{α} atoms are numbered. (b) Superposition of disulfide bridge across β-strand conformations in α-lytic protease (2ALP) 137–159, crambin (1CRN) 4–32, and β-trypsin (1TPP) 136–201. Peptide units on either side of Cys C^{α} atoms are shown. (c) Disulfide bridge across an antiparallel β-hairpin observed in the synthetic peptide Boc-Cys-Val-Aib-Ala-Leu-Cys-NHMe, and 1-1′ disulfide bridge of bis[Boc-Cys-Ala-Cys-NHMe]. (d) Superposition of the 137–159 disulfide bridge of α-lytic protease (2ALP), 1–6 disulfide bridge of Boc-Cys-Val-Aib-Ala-Leu-Cys-NHMe, and 1-1′ disulfide bridge of bis[Boc-Cys-Ala-Cys-NHMe].

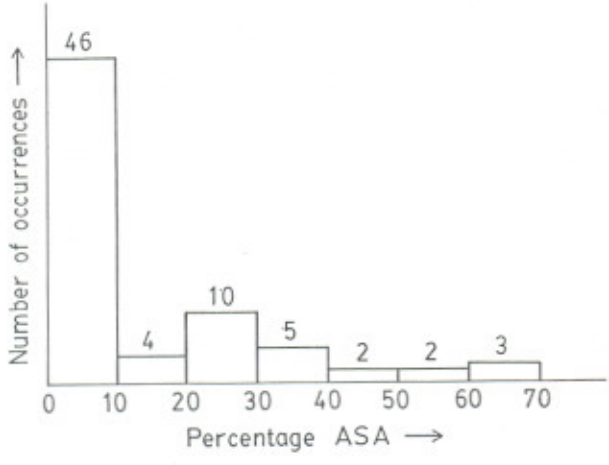

FIGURE 10

Histogram showing the distribution of the percentage accessible surface area (ASA) computed for 72 disulfide bridges in proteins.

The present analysis serves to classify disulfide bridges in proteins on the basis of their stereochemistry and permits identification of several structural classes. The results should prove useful in modelling disulfide bridges in peptides and proteins and in particular, may serve as a guide in predicting stereochemistry of new bridges introduced into proteins by site-directed mutagenesis (48).

ACKNOWLEDGMENTS

This research was supported by a grant from the Department of Science and Technology, Government of India. R.S. acknowledges the receipt of a fellowship from the Council of Scientific and Industrial Research, India.

REFERENCES

1. Thornton, J.M. (1981) *J. Mol. Biol.* **151**, 261–287
2. Creighton, T.E. (1985) *J. Phys. Chem.* **89**, 2452–2459

3. Holmgren, A. (1985) *Ann. Rev. Biochem.* **54**, 237–271
4. Creighton, T.E. (1988) *Bioessays* **8**, 57–63
5. Wetzel, R. (1987) *Trends Biochem. Sci.* **12**, 478–482
6. Wetzel, R., Perry, L.J., Baase, W.A. & Becktel, W.J. (1988) *Proc. Natl. Acad. Sci. US* **85**, 401–405
7. Matthews, B.W. (1987) *Biochemistry* **26**, 6885–6888
8. Wells, J.A. & Powers, D.B. (1986) *J. Biol. Chem.* **261**, 6564–6570
9. Katz, B.A. & Kossiakoff, A. (1986) *J. Biol. Chem.* **261**, 15480–15485
10. Villafranca, J.E., Howell, E.E., Oatley, S.J., Xuong, N.-h. & Kraut, J. (1987) *Biochemistry* **26**, 2182–2189
11. Villafranca, J.E., Howell, E.E., Voet, D.H., Strobel, M.S., Ogden, R.C., Abelson, J.N. & Kraut, J. (1983) *Science* **222**, 782–788
12. Stearman, R.S., Frankel, A.D., Freire, E., Liu, B. & Pabo, C.O. (1988) *Biochemistry* **27**, 7571–7574
13. Hruby, V.J. & Smith, C.W. (1987) in *The Peptides: Analysis, Synthesis, Biology* (Udenfriend, S. & Meienhofer, J., eds.), pp. 77–197, Academic Press, London
14. Nishiuchi, Y. & Sakakibara, S. (1982) *FEBS Lett.* **148**, 260–262
15. Yanagisawa, M., Kurihara, H., Kimura, S., Tomobe, Y., Kobayashi, M., Mitsui, Y., Yazaki, Y., Goto, K. & Masaki, T. (1988) *Nature* **332**, 411–415
16. Garičpy, J., Judd, A.K. & Schoolnik, G.K. (1987) *Proc. Natl. Acad. Sci. US* **84**, 8907–8911
17. Pabo, C.O. & Suchanek, E.G. (1986) *Biochemistry* **25**, 5987–5991
18. Hazes, B. & Dijkstra, B.W. (1988) *Protein Eng.* **2**, 119–125
19. Richardson, J.S. (1981) *Adv. Protein Chem.* **34**, 167–330
20. Bernstein, F.C., Koetzle, T.F., Williams, G.J.B., Meyer, E.F., Brice, M.D., Rodgers, J.R., Kennard, O., Shimanouchi, T. & Tasumi, M. (1977) *J. Mol. Biol.* **112**, 535–542
21. Fujinaga, M., Delbaere, L.T.J., Brayer, G.D. & James, M.N.G. (1985) *J. Mol. Biol.* **184**, 479–502
22. Norris, G.E., Anderson, B.F. & Baker, E.N. (1986) *J. Am. Chem. Soc.* **108**, 2784–2785
23. Furey, W. Jr., Wang, B.C., Yoo, C.S. & Sax, M. (1983) *J. Mol. Biol.* **167**, 661–692
24. Epp, O., Lattman, E.E., Schiffer, M., Huber, R. & Palm, W. (1975) *Biochemistry* **14**, 4943–4952
25. Teeter, M.M. (1984) *Proc. Natl. Acad. Sci. US* **81**, 6014–6018
26. Rees, D.C., Lewis, M. & Lipscomb, W.N. (1983) *J. Mol. Biol.* **168**, 367–387
27. Bourne, P.E., Sato, A., Corfield, P.W.R., Rosen, L.S., Birken, S. & Low, B.W. (1985) *European J. Biochem.* **153**, 521–527
28. Karplus, P.A. & Schulz, G.E. (1987) *J. Mol. Biol.* **195**, 701–729
29. Marquart, M., Deisenhofer, J., Huber, R. & Palm, W. (1980) *J. Mol. Biol.* **141**, 369–391
30. Dodson, E.J., Dodson, G.G., Hodgkin, D.C. & Reynolds, C.D. (1979) *Can. J. Biochem.* **57**, 469–479
31. Artymiuk, P.J. & Blake, C.C.F. (1981) *J. Mol. Biol.* **152**, 737–762
32. Bode, W., Epp, O., Huber, R., Laskowski, M. Jr. & Ardelt, W. (1985) *European J. Biochem.* **147**, 387–395
33. Kamphuis, I.G., Kalk, K.H., Swarte, M.B.A. & Drenth, J. (1984) *J. Mol. Biol.* **179**, 233–256
34. James, M.N.G. & Sielecki, A.R. (1983) *J. Mol. Biol.* **163**, 299–361
35. Dijkstra, B.W., Kalk, K.H., Hol, W.G.J. & Drenth, J. (1981) *J. Mol. Biol.* **147**, 97–123
36. James, M.N.G., Sielecki, A.R., Brayer, G.D., Delbaere, L.T.J. & Bauer, C.-A. (1980) *J. Mol. Biol.* **144**, 43–88
37. Reynolds, R.A., Remington, S.J., Weaver, L.H., Fischer, R.G., Anderson, W.F., Ammon, H.L. & Matthews, B.W. (1985) *Acta Cryst.* **B31**, 139–147
38. Wlodawer, A., Borkakoti, N., Moss, D.S. & Howlin, B. (1986) *Acta Cryst.* **B42**, 379–387
39. Almassy, R.J., J.C. Fontecilla-Camps, Suddath, F.L. & Bugg, C.E. (1983) *J. Mol. Biol.* **170**, 497–527
40. Wlodawer, A., Walter, J., Huber, R. & Sjolin, L. (1984) *J. Mol. Biol.* **180**, 307–329
41. Marquart, M., Walter, J., Deisenhofer, J., Bode, W. & Huber, R. (1983) *Acta Cryst.* **B39**, 480–490
42. Wright, C.S. (1987) *J. Mol. Biol.* **194**, 501–529
43. Bondi, A. (1964) *J. Phys. Chem.* **68**, 441–451
44. Lee, B. & Richards, F.M. (1971) *J. Mol. Biol.* **55**, 379–400
45. Ramachandran, G.N., Ramakrishnan, C. & Sasisekharan, V. (1963) *J. Mol. Biol.* **7**, 95–99
46. Karle, I.L., Kishore, R., Raghothama, S. & Balaram, P. (1988) *J. Am. Chem. Soc.* **110**, 1958–1963
47. Karle, I.L., Flippen-Anderson, J.L., Kishore, R. & Balaram, P. (1989) *Int. J. Peptide Protein Res.* **34**, 37–41
48. Sowdhamini R., Srinivasan, N., Shoichet, B., Santi, D.V., Ramakrishnan, C. & Balaram, P. (1989) *Protein Engineering* **3**, 95–103

Address:

Dr. *P. Balaram*
Molecular Biophysics Unit
Indian Institute of Science
Bangalore 560 012
India